Fe^{2+} adsorption on citrus pectin is influenced by the degree and pattern of methylesterification

Miete Celus, Clare Kyomugasho, Zahra Jamsazzadeh Kermani, Katrien Roggen, Ann M. Van Loey, Tara Grauwet and Marc E. Hendrickx*[1]

[1]Laboratory of Food Technology, Leuven Food Science and Nutrition Research Centre (LFoRCe), Department of Microbial and Molecular Systems (M^2S), KU Leuven, Kasteelpark Arenberg 22, Box 2457, 3001 Leuven, Belgium

Authors are affiliated to:

Laboratory of Food Technology
Leuven Food Science and Nutrition Research Center (LFoRCe)
Department of Microbial and Molecular Systems (M^2S)
KU Leuven
Kasteelpark Arenberg 22 box 2457
3001 Heverlee
Belgium

* Corresponding author

Telephone: +32 16 377400
E-mail: miete.celus@.kuleuven.be

Abstract

The present study aimed at gaining insight into the potential of citrus pectin to bind Fe^{2+}, a cation of great importance in a several food products. In particular the role of citrus pectin structural properties, namely the degree of methylesterification (DM) and the absolute degree of blockiness (DB_{abs} – ratio of non-methylesterified GalA units present in blocks to the total amount of GalA units) on the Fe^{2+} adsorption in aqueous solution was explored using adsorption isotherms. Demethylesterification of high DM citrus pectin enzymatically (using plant pectin methylesterase) or chemically (alkaline demethylesterification using NaOH) generated P- and C-pectins, respectively, characterized by comparable DMs but different distributions of non-methylesterified GalA units (DB_{abs}). Adsorption isotherms of P- and C-pectins in aqueous solutions of various Fe^{2+} concentrations revealed that both the DM and DB_{abs} influenced the pectin-Fe^{2+} interactions: the lower DM or higher DB_{abs}, the higher the Fe^{2+} binding capacity of citrus pectin. The Langmuir adsorption model was used to fit the experimental data for quantification of the maximum adsorption capacity (q^{G}_{max}) and the pectin-Fe^{2+} interaction energy (K_L) of the P- and C-pectins. It can be concluded that q^{G}_{max} (mol Fe^{2+}/mol GalA) was mainly determined by the DM and to a lesser extent by the DB_{abs} while the pectin-Fe^{2+} interaction energy was mainly influenced by the DB_{abs}. As a consequence, pectin modification to obtain targeted DM and DB_{abs} allows optimization of its binding capacity and therefore the associated functional properties.

Keywords

Citrus pectin, degree of methylesterification, absolute degree of blockiness, Langmuir adsorption isotherm, adsorption capacity, Fe^{2+} ions.

1. Introduction

Pectin, a major functional ingredient in the food industry, is commonly extracted from by-products of the fruit juice industry, especially apple and citrus for use as thickening or gelling

agent in sauces and jams (May, 1990; Petkowicz, Vriesmann, & Williams, 2017; Thakur, Singh, Handa, & Rao, 1997; Thibault & Ralet, 2003; Willats, Knox, & Mikkelsen, 2006). Pectin is also used in the pharmaceutical industry, as a carrier in colon-specific drug delivery systems (Liu, Fishman, & Hicks, 2006) or to reduce blood cholesterol levels (Wicker et al., 2014). These pectin functionalities, including its ability to bind divalent cations are largely related to its structural diversity (Dronnet, Renard, Axelos, & Thibault, 1996; Jamsazzadeh Kermani, Shpigelman, Pham, Van Loey, & Hendrickx, 2015; Mohnen, 2008; Willats et al., 2006). Structurally, pectin is a complex cell wall heteropolysaccharide consisting of three covalently linked building blocks, homogalacturonan (HG), rhamnogalacturonan I and II (RG I and II). HG is the predominant and linear pectin domain with a backbone consisting of α-1-4 linked galacturonic acid (GalA) residues, while RG I and II are more branched pectin domains, composed of additional monosaccharides such as rhamnose, galactose or arabinose (Caffall & Mohnen, 2009; Voragen, Coenen, Verhoef, & Schols, 2009; Yapo, Lerouge, Thibault, & Ralet, 2007).

Of particular interest in the cation binding capacity of pectin are the structural properties of the HG pectin substructure. The degree of methylesterification (DM) of pectin, which is the percentage of GalA units of HG that are methylesterified at C6, is of great importance in determining its polyanionic nature and associated functional properties (Voragen et al., 2009). It is reported that the non-methylesterified GalA residues can be negatively charged at a pH values higher than the *pKa* of pectin (3.38 – 4.10) and thereby possessing the ability to interact with divalent cations (Kyomugasho et al., 2017; Manrique & Lajolo, 2002; Sriamornsak, 2003; Thibault & Ralet, 2003). In addition to DM, the distribution pattern of non-methylesterified GalA units is hypothesized to have an important role in the cation binding capacity of pectin (Voragen et al., 2009). In fact, the DM and pattern of methylesterification have already been greatly explored in promoting pectin-Ca^{2+} interactions in context of gel formation, the more

extensive pectin application (Fraeye et al., 2009; Löfgren, Guillotin, Evenbratt, Schols, & Hermansson, 2005; Lutz, Aserin, Wicker, & Garti, 2009; Ralet, Dronnet, Buchholt, & Thibault, 2001; Slavov et al., 2009; Ström et al., 2007; Tanhatan-Nasseri, Crépeau, Thibault, & Ralet, 2011; Willats et al., 2006). According to Löfgren et al. (2005) and Ralet et al. (2001) the lower the DM and the higher the number of successive de-esterified GalA units in HG, the more sensitive the pectin chains are to Ca^{2+} cross-linking, resulting in formation of stiffer gels. Nonetheless, pectin interactions with divalent cations are not necessarily established via negatively charged carboxylic groups. Moreover, a recent study by Assifaoui et al. (2015) showed that the type of interaction between cations and pectin is also cation dependent. According to the aforementioned researchers, Zn^{2+} interacts with both the charged carboxylic group as well as with hydroxyl groups of GalA while Ca^{2+} binding occurs only via carboxylate groups. Thus, interactions between divalent cations and pectin, either with high DM, either at low pH, might occur as well as via cross-linking mechanisms other than via negatively charged carboxylic groups (Assifaoui et al., 2015; Thibault & Ralet, 2003). However, the degree and patterns of methylesterification are reported to be of major interest.

The nanostructure of pectin can be modified enzymatically or chemically to direct pectin functionality, in this context its cation binding capacity. On the one hand, enzymatic demethylesterification can be achieved by the action of pectin methylesterase (PME), which catalyses the hydrolysis of methylesters at C-6 of GalA units, resulting in negatively chargeable carboxylic groups. PMEs with an alkaline (mostly plant PME) or acidic (microbial PME) pI are distinguished. Plant PMEs are known to hydrolyse methylesters in a blockwise manner, via a single chain or multiple attack mechanism. Single chain mechanism involves hydrolysis of the methylesters until the end of the pectin chain or a blocking residue is reached prior to dissociation of the enzyme-substrate complex, whereas multiple attack mechanism describes hydrolysis of a limited average number of subsequent methylesters per enzyme attack.

Demethylesterification by microbial PMEs result in more random distributed demethylesterified GalA units (Cameron, Luzio, Goodner, & Williams, 2008; Daas, Meyer-Hansen, Schols, De Ruiter, & Voragen, 1999; Limberg et al., 2000; Ralet et al., 2001; Willats et al., 2001). On the other hand, chemical demethylesterification, which includes a treatment of pectin with alkali (sodium hydroxide), generates random distributed non methylesterified GalA units (Limberg et al., 2000). Enzymatic and chemical demethylesterification consequently result in different distributions of non-methylesterified GalA units, quantified by the degree of blockiness (DB), a concept first defined by Daas et al. (1999). The DB was established by treatment of pectin with endo-polygalacturonase followed by determination of the ratio of the amount of non-methylesterified mono-, di- and trimers released by the enzyme to the total number of non-methylesterified GalA units. Plant PME results in a higher DB than alkaline demethylesterified pectins for a given DM. In addition to the DB, the absolute degree of blockiness (DB_{abs}), which is the ratio of the amount of non-methylesterified mono-, di- and trimers released by the enzyme to the total amount of GalA units, is commonly used and expresses the absolute number of blocks of GalA in pectin (Guillotin et al., 2005). In this study, the DB_{abs} is used, given that a number of authors suggested that DB_{abs} is more informative than DB (Guillotin et al., 2005; Slavov et al., 2009; Ström et al., 2007).

Although pectin DM and DB are extensively explored in the context of gelation with Ca^{2+}, pectin has also been a subject of adsorption studies with cations other than Ca^{2+}. For instance, pectin has been explored for use in removing toxic metal ions from humans (Braudo et al., 1996; Eliaz, Hotchkiss, Fishman, & Rode, 2006; Zhao et al., 2008) or heavy metals from wastewater (Dronnet et al., 1996; Kartel, Kupchik, & Veisov, 1999; Khotimchenko, Kolenchenko, & Khotimchenko, 2008). In addition, few studies have explored the interaction between pectin and Fe^{2+}, mainly in the context of bio-accessibility (Debon & Tester, 2001; Kim, 1998; Kyomugasho et al., 2017; Miyada, Nakajima, & Ebihara, 2012). This is interesting,

given that Fe^{2+} can promote lipid oxidation in a variety of lipid based food products and that Fe^{2+} adsorption by pectin might effectively reduce lipid oxidation (Chen, McClements, & Decker, 2010; Huang, Lu, Wang, & Wu, 2011). Moreover, pectin is a dietary fiber which meets current consumer demand for natural additives (Varela & Fiszman, 2013). Fundamental insight into adsorption of Fe^{2+} by pectin could contribute to this innovative aspect. However, to the best of our knowledge, no quantitative analysis has been performed on the influence of pectin most studied structural properties, DM and DB_{abs}, on the Fe^{2+} adsorption by using adsorption isotherms.

Therefore, the present work aims at investigating the role and extent to which the DM and DB_{abs} influence the Fe^{2+} binding capacity of pectin. Given that the DM and DB_{abs} are hypothesized to influence the pectin-Fe^{2+} interaction, targeted modification of these pectin structural properties, followed by determination of the adsorption isotherms could be of great importance in exploring its Fe^{2+} binding capacity and related pectin functionalities. A better understanding of the influence of these structural factors on the Fe^{2+} adsorption could provide more insight into optimization of pectin-Fe^{2+} interactions in view of its functionalities.

2. Material and methods

2.1. Materials

High methylesterified citrus pectin, with a DM of 95%, from Sigma-Aldrich Belgium, was used as starting material for the production of pectin samples with different degrees and patterns of methylesterification. Carrots (*Daucus carota* cv. Nerac) and kiwis (*Actinidia deliciosa* cv. Hayward) were purchased from a local shop. The carrots were peeled, cut into 0.2 cm slices, frozen in liquid nitrogen and stored at -40 °C until extraction of PME. Kiwis were stored at room temperature to ripen, followed by extraction of PME inhibitor (PMEI). All chemicals used were of analytical grade. Ultrapure water (organic free, 18.2 MΩ cm resistance) was supplied

150 by a Simplicity™ water purification system (Millipore, Billerica, USA) and used for the
151 adsorption as well as analytical experiments.

152 *2.2. Preparation of pectin samples with different degrees and patterns of*
153 *methylesterification*

154 Commercial citrus pectin, mother pectin with a DM of 95.1 ± 1.8% (M95) was
155 demethylesterified to produce pectin samples with different DMs. In addition, distinct patterns
156 of methylesterification were achieved by applying different methods of demethylesterification.
157 To this extent, enzymatic or chemical demethylesterification of M95 was performed to obtain
158 blockwise or randomly distributed methylesterified GalA units, respectively (Ngouémazong et
159 al., 2011).

160 Enzymatic demethylesterification with purified plant PME was performed as described by
161 Ngouémazong et al. (2011). First, PMEI was extracted from kiwi and purified using an orange
162 PME-CNBr-Sepharose gel (Jolie et al., 2009). The purified kiwi PMEI was then coupled to an
163 NHS (N-hydroxysuccinimide)-activated Sepharose™ 4 Fast Flow matrix obtained from GE
164 Healthcare (Uppsala, Sweden). Subsequently, this gel was used to purify PME extracted from
165 carrot as described by Jolie et al. (2009). After purification, M95 (0.8% w/v in 0.1 M sodium
166 phosphate buffer pH 7) was incubated with the purified carrot PME at 30 °C for different time
167 periods. Finally, the solutions were adjusted to pH 4.5 and a 4 min thermal treatment was
168 performed at 85 °C to inactivate PME (Ngouémazong et al., 2011).

169 Chemical demethylesterification was performed according to the method of Fraeye et al.
170 (2009). Briefly, M95 was dissolved in demineralized water (0.8% w/v) and the resulting pectin
171 solution was adjusted to pH 11 with 0.1 M NaOH. Alkaline demethylesterification occurred at
172 pH 11, leading to a pH drop. The pH was kept constant at pH 11 by titration with 0.1 M NaOH.
173 The reaction was performed at 4 °C to avoid pectin depolymerisation (Fraeye et al., 2009). The

amount of NaOH added by titration to obtain a specific DM was theoretically determined based on the stoichiometry of the alkaline demethylesterification reaction (Ngouémazong et al., 2011). After addition of the predetermined amounts of NaOH, the demethylesterification was stopped by adjusting the pH to 4.5 (Fraeye et al., 2009).

Subsequently, the enzymatically and chemically demethylesterified pectin samples were adjusted to pH 6, dialyzed (Spectra/Por®, MWCO = 12-14 kDa) for 48 h against demineralized water and lyophilized. For further use, the enzymatically demethylesterified pectins will be denoted as P-pectins while the chemically demethylesterified pectins will be denoted as C-pectins.

2.3. Characterization of the pectin samples

2.3.1. Degree of methylesterification, GalA content, molar mass distribution and intrinsic cation concentration of the pectin samples

All pectin samples were characterized for their degree of methylesterification, GalA content, molar mass distribution and intrinsic cation concentrations.

Measurement of the DM was performed using Fourier transform infra-red (FT-IR) (Shimadzu FTIR-8400S, Japan) according to the method described by Kyomugasho et al. (2015a). A standard curve without deconvolution of the spectra was used (Kyomugasho et al., 2015a).

To measure the GalA content, pectin samples were first hydrolyzed with concentrated sulfuric acid according to the method described by Ahmed & Labavitch (1977). The GalA concentration of the hydrolyzed samples was then quantified by a spectrophotometric method as described by Blumenkrantz & Asboe-Hansen (1973). The hydrolysis was performed in duplicate.

Molar mass distributions of the pectin samples were assessed as described by Shpigelman, Kyomugasho, Christiaens, Van Loey, & Hendrickx (2014) in order to ensure that no depolymerisation occurred during the demethylesterification step. High-performance size

198 exclusion chromatography (HPSEC) coupled to a refractive index (RI) detector (Shodex RI-
199 101, Showa Denko K.K., Kawasaki, Japan), a multi-angle laser light scattering detector
200 (MALLS) (PN3621, Postnova Analytics, Landsberg am Lech, Germany), diode array detector
201 (Agilent Technologies, Santa Clara, CA, USA) and a viscometer (PN3310, Postnova analytics,
202 Landsberg am Lech, Germany) was used. Exactly 100 µl of filtered 0.2% (w/v) pectin solutions
203 was injected onto a series of Waters columns at 35 °C (Waters, Milford, MA), namely Ultra
204 hydrogel 250, 1000 and 2000 with exclusion limits of 8 x 10^4, 4 x 10^6 and 1 x 10^7 g/mol,
205 respectively. A 0.1 M acetic acid buffer (pH 4.4) with 0.1 M $NaNO_3$ was used for elution at a
206 flow rate of 0.5 mL/min. The weight average molar mass was then calculated using the Debye
207 fitting method (2^{nd} order) of the software provided by the manufacturer of the MALLS detector
208 and a *dn/dc* value of 0.146 mL/g was used for all samples.

209 The concentration of intrinsic cations in the pectin samples was measured by inductively
210 coupled plasma mass spectrometry (ICP-MS). Before analysis, pectin samples were incinerated
211 in a muffle furnace at 550 °C for 22 h and further treated as described by Kyomugasho,
212 Willemsen, Christiaens, Van Loey, & Hendrickx (2015b). The analysis was performed using
213 an Agilent 7700x ICP-MS (Agilent Technologies, Santa Clara, CA, USA). The concentrations
214 of ^{24}Mg, ^{44}Ca, ^{56}Fe and ^{66}Zn were measured in helium mode using ^{72}Ge as an internal standard.
215 The cations were quantified using reference standard solutions with certified concentrations
216 (Kyomugasho et al., 2015b).

217 *2.4. Estimation of the absolute degree of blockiness*

218 The pattern of methylesterification of the pectin samples can be quantified by the degree of
219 blockiness (DB) or absolute degree of blockiness (DB_{abs}). The DB is the ratio of the number of
220 non-methylesterified GalA units present in blocks to the total non-methylesterified GalA units
221 (Daas et al., 1999), whereas DB_{abs} is defined as the ratio of non-methylesterified GalA units
222 present in blocks to the total amount of GalA units (Guillotin et al., 2005). In this study, only

223 DB_{abs} is taken into account and was predicted based on parameter estimates of polynomial
224 functions determined by Ngouémazong et al. (2011). The use of these polynomial equations is
225 justified, given that the present study used exactly the same procedures and materials for the
226 targeted pectin modification as described by Ngouémazong et al. (2011). The polynomial
227 functions used are achieved by Ngouémazong et al. (2011) by relating DB_{abs} to DM of tailored
228 pectin samples and are described as follows:

229 P-pectins: $DB_{abs} = 0.472\ (\pm 0.03)\ DM^2 - 1.485\ (\pm 0.04)\ DM + 1.009$

230 C-pectins: $DB_{abs} = -1.998\ (\pm 0.10)\ DM^3 + 4.595\ (\pm 0.20)\ DM^2 - 3.598\ (\pm 0.06)\ DM + 1.000$

231 *2.5. Experimental determination of Fe^{2+} adsorption isotherms of the pectin samples*

232 An adsorption equilibrium study was performed based on the method of Debon & Tester (2001)
233 to determine the Fe^{2+} adsorption capacity of pectin and specifically the relation between the
234 Fe^{2+} adsorption capacity and pectin DM and DB_{abs}. Therefore, deaerated aqueous solutions (10
235 mL) of the pectin samples (0.1% w/v) were enriched with 0 to 3.6 mM Fe^{2+} and subsequently
236 transferred to previously rinsed dialysis membranes (Spectra/Por®, MWCO = 3.5 kDa). These
237 membranes were equilibrated in closed jars containing 50 mL deaerated ultrapure water, which
238 was constantly stirred. The jars were placed in a pharmaceutical refrigerator (MPR-311D (H),
239 Sanyo Electric Biomedical Co., Tokyo, Japan) at 15 °C for 48 h until an equilibrium between
240 nonbound Fe^{2+} inside and outside the membrane was achieved. The period of 48 h was
241 determined in a series of preliminary experiments analyzing the Fe^{2+} concentration as a function
242 of time. In addition to the use of deaerated water, the experiment was performed in a nitrogen
243 atmosphere using a pyramid portable glove bag (Erlab, Val de Reuil, France), installed in the
244 refrigerator to avoid an oxygen-rich atmosphere, hence Fe^{2+} oxidation. After equilibration, the
245 Fe^{2+} concentration of the outside solution was measured spectrophotometrically according to
246 Viollier, Inglett, Hunter, Roychoudhury, & Van Capellen (2000) with some minor

modifications. An aliquot of the outside solution (1 mL) was transferred into a cuvette with the addition of 100µl of 0.01 M ferrozine (3-(2-pyridyl)-5,6-diphenyl-1,2,4-triazine-*p*,*p*'-disulfonic acid monosodium salt hydrate) and 50µl of 5 M ammonium acetate buffer (pH 9.5). After 5 min, the absorbance was measured at 562 nm (1800 UV spectrophotometer, Shimadzu, Kyoto, Japan). The analysis was performed in triplicate and the Fe^{2+} concentration was determined using a standard curve of $FeSO_4$ solutions (0-0.1 mM). The Fe^{2+} adsorption capacity (q_e) of pectin was estimated based on the difference between the initial Fe^{2+}concentration and the concentration measured after equilibrium and calculated as follows (Khotimchenko et al., 2008):

$$q_e \left(\frac{mol\ Fe^{2+}}{mol\ GalA}\right) = \frac{[(C_0\ .\ V_{in} - C_e\ .\ (V_{in} + V_{out})]}{n_{GalA}}$$

with C_0, the initial Fe^{2+} concentration (mM), C_e, the Fe^{2+}concentration at equilibrium (mM), V_{in} and V_{out}, the volume inside (10 mL) and outside (50 mL) the dialysis membrane, respectively and n_{GalA} represents the absolute amount of GalA units in the pectin sample (mol). Taking into account the DM of the pectin sample, q_e can be expressed as mol Fe^{2+}/mol COO^- as well.

Since the adsorption equilibrium studies were performed at a constant temperature, adsorption isotherms indicating the amount of Fe^{2+} bound to each GalA or COO^- unit (q_e) as a function of the Fe^{2+} concentration at equilibrium (C_e) were obtained

2.6. Data analysis of Fe^{2+} adsorption isotherms of the pectin samples

The adsorption isotherms of the pectin samples obtained can be quantitatively described by several empirical models such as the Langmuir, Freundlich, Brunauer-Emmett-Teller (BET), BiLangmuir or Redlich-Peterson adsorption isotherm (Foo & Hameed, 2010; Ho, Huang, & Huang, 2002; Khotimchenko et al., 2008; Zhao, Repo, Yin, & Sillanpää, 2013). Such isotherms are typically characterized by certain parameters, which indicate surface properties of the

adsorbent and the adsorption affinity (Ho et al., 2002). The Langmuir isotherm, which is the most widely used adsorption isotherm, assumes monolayer adsorption at homogenous and finite binding sites within an adsorbent and is represented as (Chen, 2015; Ho et al., 2002; Schmuhl, Krieg, & Keizer, 2001):

$$q_e = \frac{q_{max} \cdot K_L \cdot C_e}{1 + K_L \cdot C_e}$$

with q_{max} as the maximum adsorption capacity at the monolayer (mol Fe^{2+}/mol GalA or mol Fe^{2+}/mol COO^-), q_e, the adsorption capacity of a GalA or COO^- unit (mol Fe^{2+}/mol GalA or mol Fe^{2+}/mol COO^-) belonging to an Fe^{2+} equilibrium concentration, K_L, the Langmuir constant (L/mmol Fe^{2+}), which is a measure of the interaction energy and C_e, the Fe^{2+} equilibrium concentration (mmol Fe^{2+}/L).

Besides the Langmuir isotherm, the Freundlich isotherm was also employed in this study and assumes heterogeneous, reversible and multilayer adsorption (Chen, 2015; Schmuhl et al., 2001; Zhao et al., 2013):

$$q_e = K_F \, x \, C_e^{1/n}$$

with K_F ((mol/mol GalA)(L/mmol)$^{1/n}$), the Freundlich constant and n, the Freundlich parameter related to the degree of heterogeneity of the system (Zhao et al., 2013).

Modeling of the experimental data of the pectin samples by both Langmuir and Freundlich adsorption isotherms was performed using non-linear one step regression (SAS version 9.4, Cary, North Carolina).

2.7. Statistical analysis

Differences in experimental data were analyzed using the statistical software JMP (JMP 13, SAS Institute Inc., Cary, NC, USA) and the Tukey's studentized range post-hoc test was carried

293 out to analyze significant differences with a 95% confidence interval ($p < 0.05$) between the
294 experimental data.

295 **3. Results and discussion**

296 *3.1. Characterization of the pectin samples*

297 *3.1.1. GalA content, weight average molar mass and intrinsic cation concentration of the*
298 *pectin samples*

299 The GalA content of all pectin samples was similar (average: 0.747 ± 0.050 g GalA/g pectin).
300 The intrinsic cation concentrations of the pectin samples were also analyzed and the results
301 indicated highest concentrations for Mg^{2+} and Ca^{2+} (0.2 - 1.0 mg/g pectin). Intrinsic iron (sum
302 of Fe^{2+} and Fe^{3+}) was present in clearly lower concentrations, not exceeding 59 µg/g of pectin.
303 As such, these cation concentrations were too low to interfere with the adsorption of Fe^{2+}. The
304 observed results of pectin-Fe^{2+} adsorption capacities can therefore be largely attributed to the
305 cations added.
306 In the case of molar mass, the different pectin samples revealed similar distributions and
307 comparable weight average molar masses, varying between 41 and 66 kDa. This evidences that
308 no depolymerisation occurred during the demethylesterification reactions which is in agreement
309 with the observations of Fraeye et al. (2009), Kim & Wicker (2009), Ngouémazong et al. (2011)
310 and Tanhatan-Nasseri et al. (2011).

311 *3.1.2. Degree and pattern of methylesterification of the pectin samples*

312 Starting from the mother pectin (M95), tailored pectins with distinct DMs were obtained via
313 enzymatic (P-pectins) and chemical (C-pectins) demethylesterification. For both P- and C-
314 pectins similar DM values were intended as shown in **Table 1**. Since no depolymerisation
315 occurred during this demethylesterification and given that the demethylesterification methods
316 generated pectins with different patterns of methylesterification, P- and C-pectin samples with
317 a similar DM were expected to only differ in the DB_{abs} (**Table 1**). The DB_{abs} is a measure of the

318 percentage of non-methylesterified GalA units present in blocks in the entire pectin population
319 (Guillotin et al., 2005). In other words, a high DB_{abs} implies a high number of blocks of
320 successive non-methylesterified GalA units. For the mother pectin sample (M95) a DB_{abs} of <
321 0.74% was established as this value corresponds to the detection limit of the method used to
322 obtain experimental DB_{abs} values on which the polynomial functions are based (Ngouémazong
323 et al., 2011). In general, the DB_{abs} was expected to increase with decreasing DM for both P-
324 and C-pectins, indicating a higher number of blocks of successive non-methylesterified GalA
325 units at lower DM, since lowering the DM resulted in an increased number of non-
326 methylesterified GalA units (**Table 1**). At a given DM, a lower DB_{abs} was estimated for the C-
327 pectins compared to the P-pectins due to the random demethylesterification of the former. In
328 other words, P-pectins showed more blocks of successive non-methylesterified GalA units than
329 the C-pectins. The estimated DB_{abs} values from this study are comparable with those of other
330 studies (Ström et al., 2007; Tanhatan-Nasseri et al., 2011). Regarding the alkaline
331 demethylesterified pectin samples, the estimated DB_{abs} values in the present study were very
332 similar to DB_{abs} values reported in literature. For instance, the present study estimated a DB_{abs}
333 of 12.3 ± 0.3% and 43.9 ± 0.9% for C-pectins with DM of 46 and 20%, respectively, whereas
334 chemically demethylesterified pectin samples of other studies with similar DMs (45 and 20%)
335 were characterized by a DB_{abs} of 16 and 44%, respectively (Ström et al., 2007; Tanhatan-
336 Nasseri et al., 2011). The estimated DB_{abs} values of the majority of the enzymatical
337 demethylesterified pectin samples were also comparable with values from studies of Ström et
338 al. (2007) and Tanhatan-Nasseri et al. (2011). These authors observed DB_{abs} values of 27, 29
339 and 56% for enzymatic (plant PME) demethylesterified pectin samples with DMs of 70, 60 and
340 40%, respectively, whereas in the present study DB_{abs} values of 20.6 ± 1.0% (P69), 29.0 ± 1.3%
341 (P60) and 49.9 ± 1.0% (P39) were estimated for pectins with similar DMs. Some discrepancies

were observed, mostly at lower DMs, but those can be attributed to different pectin and PME sources (Ngouémazong et al., 2011).

3.2. Fe^{2+} adsorption isotherms of the pectin samples

Adsorption isotherms of the differently demethylesterified citrus pectin samples were obtained to determine their binding capacity of Fe^{2+} and the relation between this Fe^{2+} binding capacity and pectin DM as well as DB_{abs}. From the adsorption isotherms of the P- and C-pectins shown in **Fig. 1**, it can be observed that the adsorption capacity (mol Fe^{2+}/mol GalA) of all samples increased with increasing equilibrium Fe^{2+}concentration until a maximum was reached. This plateau indicates saturation and represents the maximum amount of Fe^{2+} that can be bound to the pectin sample (q_{max}) (Schmuhl et al., 2001; Zhao et al., 2013). The experimental data of the majority of the pectin samples were better described by the Langmuir adsorption model, with $R^2_{adjusted}$ values ≥ 0.98 as shown in **Table 2,** than the Freundlich model. The use of the Langmuir adsorption isotherm implies that demethylesterified citrus pectin contains a limited number of homogeneous binding sites and Fe^{2+} binding occurred via monolayer adsorption with a constant adsorption energy distribution (Foo & Hameed, 2010; Schmuhl et al., 2001; Zhao et al., 2013). The estimated parameters of the Langmuir adsorption isotherm are shown in **Table 2**, in which the maximum Fe^{2+} adsorption capacity expressed as mol Fe^{2+}/mol GalA is indicated as q^G_{max} while the maximum amount of Fe^{2+} bound to each mole of COO^- is represented as q^C_{max}.

As presented in **Table 2** and **Fig. 1**, the DM had a clear influence on the Fe^{2+} adsorption capacity of both P- and C-pectins. In general, the maximum adsorption capacities, expressed in mol Fe^{2+}/mol GalA (q^G_{max}), of both P- and C-pectins increased significantly ($p < 0.05$) with decreasing DM. For instance, mother pectin M95, could bind 0.217 ± 0.005 mol Fe^{2+}/mol GalA, while P13 and C20 revealed q^G_{max} values of 0.523 ± 0.010 and 0.427 ± 0.009 mol Fe^{2+}/mol GalA, respectively. This observation can be attributed to the higher number of negatively chargeable carboxylic groups in pectin samples with lower DM. The results of this study are in agreement

with the findings of Khotimchencko et al. (2008), who observed that decreasing the DM of citrus pectin promoted the Zn^{2+} adsorption capacity. The data of the aforementioned researchers were also modeled by the Langmuir adsorption isotherm. In the case of C-pectins of the present study, one exception was observed where C67 bound significantly less Fe^{2+} than M95, with 0.191 ± 0.004 compared to 0.217 ± 0.005 mol Fe^{2+}/mol GalA, respectively (**Table 2**). Despite exhibiting a lower DM value, the random demethylesterification did not necessarily increase the sensitivity of C67 to Fe^{2+} due to the limited blocks of chargeable non-methylesterified GalA residues. Consequently, C67 and M95 exhibited comparable and low DB_{abs} values, which probably explains the comparable maximum adsorption capacities. Moreover, it evidences that a certain number of blocks (DB_{abs} > 5.1 ± 0.1 %, **Table 1**) has to be achieved before pectin-Fe^{2+} interactions occurred. This observation is in comparison with reported pectin-Ca^{2+} interactions, where in general at least six to ten consecutive non-methylesterified GalA units are required along the pectin chain for formation of stable junction zones with Ca^{2+} (Luzio & Cameron, 2008; Ngouémazong et al., 2012; Thakur et al., 1997; Voragen et al., 2009).

More insight into the role of pectin DM and DB_{abs} on the Fe^{2+} adsorption capacity was obtained by comparing the q^{G}_{max} values of P- and C- pectins among each other. In **Fig. 2a**, q^{G}_{max} values are plotted in function of the DM (%) and estimated DB_{abs} (%). It should be noted that within this three dimensional space, not every combination of DM and DB_{abs} is possible, given the methods used, as a DB_{abs} value is always related with a given DM. From **Fig. 2a**, it is clear that q^{G}_{max} values increased with decreasing DM and/or increasing DB_{abs} for both P- and C-pectins. This implies that pectin with both a higher number as more consecutive negative chargeable non-methylesterified GalA units bound more Fe^{2+}. However, from a DB_{abs} of approximately 44%, only little further increase in the maximum adsorption capacity occurred, implying that an increase of blocks of negatively chargeable carboxylic groups beyond 44% did not necessarily

lead to more Fe^{2+} binding. Irani, Owen, Mercadante & Williams (2017) also observed that maximum 40% of the galacturonic acid residues, present in blocks, was bound to counterions.

For a given DM, the P-pectins showed generally significantly ($p < 0.05$) higher q^{G}_{max} values than the C-pectins, which is illustrated in **Fig. 2b**. For instance, for P39 and C36, both pectin samples with similar DM, q^{G}_{max} values of 0.429 ± 0.015 and 0.372 ± 0.011 mol Fe^{2+}/mol GalA, respectively, were observed. This difference in q^{G}_{max} between the P- and C pectins for a given DM could be largely attributed to the higher DB_{abs} of the P-pectins. In addition, higher maximum adsorption capacities were observed for C-pectins compared to P-pectins of the same DB_{abs} (**Fig. 2a**), with 0.309 ± 0.006 mol Fe^{2+}/mol GalA for P60 (DB_{abs} of 29.0 ± 1.3%) and 0.372 mol Fe^{2+}/mol GalA for C36 (DB_{abs} of 28.1 ± 0.4%), which is explained by the lower DM for the C-pectins. Although both structural parameters (DM and DB_{abs}) influenced the Fe^{2+} binding capacity of pectin, it can be concluded that the DM is more determining the maximum Fe^{2+} adsorption capacity of pectin than the DB_{abs}. Samples with a similar DM (A on **Fig. 2a**) exhibited smaller differences in q^{G}_{max} value (A' on **Fig. 2a**) than samples with a similar DB_{abs} (B and B' on **Fig. 2a**). In other words, the number of negative charges had a larger influence on the amount of Fe^{2+} that can be bound, compared to the consecutiveness of these negative charges. The conclusion of the present study that both the DM and DB_{abs} of citrus pectin influenced the Fe^{2+} binding capacity is in accordance with the results of Irani et al. (2017), who concluded that HG with a decreased DM and high blockwise distributed charged carboxylic groups could exhibit local counterion condensation.

The estimated Langmuir constant (K_L) is related to the affinity between pectin and Fe^{2+} and is considered as a measure of the interaction energy (Khotimchenko et al., 2008). The K_L value (L/mmol Fe^{2+}) increased proportionally with decreasing DM and increasing DB_{abs} for both P- and C-pectins, which can be seen in **Table 2** and **Fig. 3a**. This observation indicates stronger pectin-Fe^{2+} interactions with an increasing number of (consecutive) negative charges.

Moreover, a sharp increase of K_L was observed between pectin samples with a DB_{abs} of 43.9 ± 0.9% (C20) and 49.9± 1.0% (P39), which evidences that the pectin-Fe^{2+} interaction was clearly stronger when pectin exhibited more (blocks of) successive negative chargeable GalA units (DB_{abs} > 44%) (**Fig. 3a**). However, beyond this increase, particularly for DB_{abs} values higher than 49%, no significant ($p > 0.05$) increase in K_L value was observed (**Fig. 3a**), indicating that a further increase of the DB_{abs} did not lead to stronger pectin-Fe^{2+} interactions. **Fig. 3b** illustrates significant ($p < 0.05$) differences in K_L values between the P- and C-pectins with similar DMs, which might be explained by the higher DB_{abs} values for P-pectins compared to C-pectins as P39 (DB_{abs} of 49.9 ± 1.0 %) exhibited a value of 473.6 ± 104.1 L/mmol Fe^{2+}, whereas C36 (DB_{abs} of 20.8 ± 0.8 %) showed a K_L value of 128.8 ± 23.3 L/mmol Fe^{2+}. Therefore, pectin with a given DM and higher DB_{abs} values interacted stronger with Fe^{2+}, which is in analogy with the reported studies of pectin-Ca^{2+} interactions (Fraeye et al., 2009; Löfgren et al., 2005; Ralet et al., 2001). In contrast, no clear differences in K_L values were observed between P- and C-pectins of a given DB_{abs} (**Fig. 3a**). As a result, it can be concluded that the pectin-Fe^{2+} interaction energy is determined by the DB_{abs}. The DM did not largely influence the Fe^{2+} affinity for pectin with a given DB_{abs}.

Finally, in **Table 2** the moles of Fe^{2+} bound to each mole of COO^- for the different pectin samples are shown (q^C_{max}). The highly methylesterified mother pectin (M95) revealed an exceptionally high value, which probably implies binding of Fe^{2+} to functional groups of pectin, other than COO-, such as hydroxyl groups as proposed for Zn^{2+} (Assifaoui et al., 2015). Nevertheless, low DM pectins also contain hydroxyl groups but probably showed higher sensitivity for ionic interaction via negatively chargeable carboxylic groups. **Fig. 4** presents the q^C_{max} values (mol Fe^{2+}/mol COO^-) as a function of the DM (%), fitted by a linear equation (q^C_{max} = a x DM + b). The q^C_{max} value of M95 is removed to clearly visualize the differences between the P- and C-pectins. The q^C_{max} values exhibited by the C-pectins were not significantly different

441 ($p > 0.05$) and were characterized by a linear curve with a slope not significantly different ($p >$
442 0.05) from zero. In addition, the q_{max}^{C} values of the C-pectins were approximately 0.5 mol
443 Fe^{2+}/mol COO^-, which implies an ionic interaction of two moles of COO^- with one mole of Fe^{2+}
444 and suggests egg-box model binding as described for Ca^{2+} (Grant, Morris, Rees, Smith, &
445 Thom, 1973). The P-pectins exhibited an increase in adsorption capacity with increasing DM,
446 with a slope significantly ($p < 0.05$) higher than that of the C-pectins. For a given DM, this
447 implies that significantly higher amounts of Fe^{2+} are bound to negatively charged carboxylic
448 groups of pectin with a higher DB_{abs} (P-pectins compared to C-pectins) or that other interactions
449 than via COO^- were possible. It is noteworthy that the estimated parameters of the intercept of
450 both P- and C-pectins are not significantly different, indicating that the amount of Fe^{2+} bound
451 to each mole of COO^- is similar at very low DM or in other words, when DB_{abs} is comparable
452 between the P- and C-pectins.

453 **Conclusion**

454 This research explored the relation between structural properties of citrus pectin, in particular
455 the DM and DB_{abs}, and its Fe^{2+} adsorption capacity. The adsorption isotherms obtained were
456 well described by the Langmuir adsorption model. The results of this study revealed a
457 dependence of the Fe^{2+} adsorption of citrus pectin on both pectin DM and DB_{abs}. A high Fe^{2+}
458 binding capacity was exhibited by low DM pectin due to the presence of a higher number of
459 negatively chargeable carboxylic groups, and by a higher number of blocks of successive non-
460 methylesterified GalA units (high DB_{abs}). In addition, the maximum adsorption capacity was
461 mainly determined by the DM while the pectin-Fe^{2+} interaction energy was predominantly
462 influenced by the DB_{abs} of citrus pectin. These results suggest that targeted modification of
463 pectin DM and DB_{abs} can be applied to derive desired functionality, particularly cation binding
464 capacity. Depending on the intended application, pectin structural properties can be directed to
465 obtain high Fe^{2+} binding capacities, for use as a better gelling agent or antioxidant, as well as

low Fe^{2+} binding abilities, in the context of mineral bio-accessibility. Moreover, these results could form the basis for exploring pectin *in situ* for its cation binding capacity. By targeted processing of fruits and vegetables, pectin can be structurally modified to obtain desired cation binding properties, without addition of externally modified pectin as an ingredient.

Acknowledgements

The authors acknowledge the financial support of the KU Leuven Research Council (METH/14/03) through the long term structural funding-Methusalem funding by the Flemish Government. Miete Celus is a Ph.D. Fellow funded by the agency for innovation by science and technology (IWT) (Grant no. 141440). C. Kyomugasho is a postdoctoral researcher funded by the Onderzoeksfonds KU Leuven post-doctoral fellowship (PDM).

References

Ahmed, A. E. R., & Labavitch, J. M. (1977). A simplified method for accurate determination of cell wall uronide content. *Journal of Food Biochemistry*, *1*, 361–365.

Assifaoui, A., Lerbret, A., Uyen, H. T. D., Neiers, F., Chambin, O., Loupiac, C., & Cousin, F. (2015). Structural behaviour differences in low methoxy pectin solutions in the presence of divalent cations ($Ca^{2+}$and Zn^{2+}): a process driven by the binding mechanism of the cation with the galacturonate unit. *Soft Matter*, *11*, 551–560.

Blumenkrantz, N., & Asboe-Hansen, G. (1973). New method for quantitative determination of uronic acids. *Analytical Biochemistry*, *54*, 484–489.

Braudo, E. E., Danilova, I. V., Dianova, V. T., Kobak, V. V., Plashchina, I. G., Sidorov, E. V., & Bogatyrev, A. N. (1996). Thermodynamic approach to the selection of polyuronide sequestrants for preventive and medicinal nutrition. *Die Nahrung*, *40*, 205–8.

Caffall, K. H., & Mohnen, D. (2009). The structure, function, and biosynthesis of plant cell wall pectic polysaccharides. *Carbohydrate Research*, *344*, 1879–1900.

Cameron, R. G., Luzio, G. A., Goodner, K., & Williams, M. A. K. (2008). Demethylation of a model homogalacturonan with a salt-independent pectin methylesterase from citrus: I. Effect of pH on demethylated block size, block number and enzyme mode of action. *Carbohydrate Polymers*, *71*(2), 287–299.

494 Chen, B., McClements, D. J., & Decker, E. A. (2010). Role of continuous phase anionic
495 polysaccharides on the oxidative stability of menhaden oil-in-water emulsions. *Journal of*
496 *Agricultural and Food Chemistry*, *58*, 3779–3784.

497 Chen, X. (2015). Modeling of experimental adsorption isotherm data. *Information*
498 *(Switzerland)*, *6*, 14–22.

499 Daas, P. J. H., Meyer-Hansen, K., Schols, H. A., De Ruiter, G. A., & Voragen, A. G. J. (1999).
500 Investigation of the non-esterified galacturonic acid distribution in pectin with
501 endopolygalacturonase. *Carbohydrate Research*, *318*, 135–145.

502 Debon, S. J. J., & Tester, R. F. (2001). In vitro binding of calcium, iron and zinc by non-starch
503 polysaccharides. *Food Chemistry*, *73*, 401–410.

504 Dronnet, V. M., Renard, C. M. G. C., Axelos, M. A. V, & Thibault, J. F. (1996).
505 Characterisation and selectivity of divalent metal ions binding by citrus and sugar-beet
506 pectins. *Carbohydrate Polymers*, *30*, 253–263.

507 Eliaz, I., Hotchkiss, A. T., Fishman, M. L., & Rode, D. (2006). The effect of modified citrus
508 pectin on urinary excretion of toxic elements. *Phytotherapy Research*, *20*, 859–864.

509 Foo, K. Y., & Hameed, B. H. (2010). Insights into the modeling of adsorption isotherm systems.
510 *Chemical Engineering Journal*, *156*, 2–10.

511 Fraeye, I., Doungla, E., Duvetter, T., Moldenaers, P., Van Loey, A., & Hendrickx, M. (2009).
512 Influence of intrinsic and extrinsic factors on rheology of pectin-calcium gels. *Food*
513 *Hydrocolloids*, *23*, 2069–2077.

514 Grant, G. T., Morris, E. R., Rees, D. A., Smith, P. J. C., & Thom, D. (1973). Biological
515 interactions between polysaccharides and divalent cations: the egg-box model. *FEBS*
516 *Letters*, *32*, 195–198.

517 Guillotin, S. E., Bakx, E. J., Boulenguer, P., Mazoyer, J., Schols, H. A., & Voragen, A. G. J.
518 (2005). Populations having different GalA blocks characteristics are present in commercial
519 pectins which are chemically similar but have different functionalities. *Carbohydrate*
520 *Polymers*, *60*, 391–398.

521 Ho, Y. S., Huang, C. T., & Huang, H. W. (2002). Equilibrium sorption isotherm for metal ions
522 on tree fern. *Process Biochemistry*, *37*, 1421–1430.

Huang, P. H., Lu, H. T., Wang, Y. T., & Wu, M. C. (2011). Antioxidant activity and emulsion-stabilizing effect of pectic enzyme treated pectin in soy protein isolate-stabilized oil/water emulsion. *Journal of Agricultural and Food Chemistry*, *59*, 9623–9628.

Irani, A. H., Owen, J. L., Mercadante, D., & Williams, M. A. K. (2017). Molecular dynamics simulations illuminate the role of counterion condensation in the electrophoretic transport of homogalacturonans. *Biomacromolecules*, *18*(2), 505–516.

Jamsazzadeh Kermani, Z., Shpigelman, A., Pham, H. T. T., Van Loey, A. M., & Hendrickx, M. E. (2015). Functional properties of citric acid extracted mango peel pectin as related to its chemical structure. *Food Hydrocolloids*, *44*, 424–434.

Jolie, R. P., Duvetter, T., Houben, K., Clynen, E., Sila, D. N., Van Loey, A. M., & Hendrickx, M. E. (2009). Carrot pectin methylesterase and its inhibitor from kiwi fruit: Study of activity, stability and inhibition. *Innovative Food Science and Emerging Technologies*, *10*, 601–609.

Kartel, M. T., Kupchik, L. A., & Veisov, B. K. (1999). Evaluation of pectin binding of heavy metal ions in aqueous solutions. *Chemosphere*, *38*, 2591–2596.

Khotimchenko, M. Y., Kolenchenko, E. A., & Khotimchenko, Y. S. (2008). Zinc-binding activity of different pectin compounds in aqueous solutions. *Journal of Colloid and Interface Science*, *323*, 216–222.

Kim, M. (1998). Highly esterified pectin with low molecular weight enhances intestinal solubility and absorption of ferric iron in rats. *Nutrition Research*, *18*, 1981–1994.

Kim, Y., & Wicker, L. (2009). Valencia PME isozymes create charge modified pectins with distinct calcium sensitivity and rheological properties. *Food Hydrocolloids*, *23*(3), 957–963.

Kyomugasho, C., Christiaens, S., Shpigelman, A., Van Loey, A. M., & Hendrickx, M. E. (2015). FT-IR spectroscopy, a reliable method for routine analysis of the degree of methylesterification of pectin in different fruit- and vegetable-based matrices. *Food Chemistry*, *176*, 82–90.

Kyomugasho, C., Gwala, S., Christiaens, S., Jamsazzadeh Kermani, Z., Van Loey, A. M., Grauwet, T., & Hendrickx, M. E. (2017). Pectin nanostructure influences pectin-cation interactions and in vitro-bioaccessibility of Ca^{2+}, Zn^{2+}, Fe^{2+} and Mg^{2+}-ions in model

systems. *Food Hydrocolloids*, *62*, 299–310.

Kyomugasho, C., Willemsen, K. L. D. D., Christiaens, S., Van Loey, A. M., & Hendrickx, M. E. (2015). Pectin-interactions and invitro bioaccessibility of calcium and iron in particulated tomato-based suspensions. *Food Hydrocolloids*, *49*, 164–175.

Limberg, G., Körner, R., Buchholt, H. C., Christensen, T. M. I. E., Roepstorff, P., & Mikkelsen, J. D. (2000). Analysis of different de-esterification mechanisms for pectin by enzymatic fingerprinting using endopectin lyase and endopolygalacturonase II from A. Niger. *Carbohydrate Research*, *327*(3), 293–307.

Liu, L., Fishman, M. L., & Hicks, K. B. (2006). Pectin in controlled drug delivery – a review. *Cellulose*, *14*(1), 15–24.

Löfgren, C., Guillotin, S., Evenbratt, H., Schols, H., & Hermansson, A. M. (2005). Effects of calcium, pH, and blockiness on kinetic rheological behavior and microstructure of HM pectin gels. *Biomacromolecules*, *6*(2), 646–652.

Lutz, R., Aserin, A., Wicker, L., & Garti, N. (2009). Structure and physical properties of pectins with block-wise distribution of carboxylic acid groups. *Food Hydrocolloids*, *23*(3), 786–794.

Luzio, G. A., & Cameron, R. G. (2008). Demethylation of a model homogalacturonan with the salt-independent pectin methylesterase from citrus: Part II. Structure-function analysis. *Carbohydrate Polymers*, *71*(2), 300–309.

Manrique, G. D., & Lajolo, F. M. (2002). FT-IR spectroscopy as a tool for measuring degree of methyl esterification in pectins isolated from ripening papaya fruit. *Postharvest Biology and Technology*, *25*, 99–107.

May, C. D. (1990). Industrial pectins: Sources, production and applications. *Carbohydrate Polymers*, *12*, 79–99.

Miyada, T., Nakajima, A., & Ebihara, K. (2012). Degradation of pectin in the caecum contributes to bioavailability of iron in rats. *The British Journal of Nutrition*, *107*, 1452–1457.

Mohnen, D. (2008). Pectin structure and biosynthesis. *Current Opinion in Plant Biology*, *11*, 266–277.

582 Ngouémazong, D. E., Tengweh, F. F., Duvetter, T., Fraeye, I., Van Loey, A., Moldenaers, P.,
583 & Hendrickx, M. (2011). Quantifying structural characteristics of partially de-esterified
584 pectins. *Food Hydrocolloids*, *25*, 434–443.

585 Ngouémazong, D. E., Tengweh, F. F., Fraeye, I., Duvetter, T., Cardinaels, R., Van Loey, A.,
586 … Hendrickx, M. (2012). Effect of de-methylesterification on network development and
587 nature of Ca2+-pectin gels: Towards understanding structure-function relations of pectin.
588 *Food Hydrocolloids*, *26*, 89–98.

589 Petkowicz, C. L. O., Vriesmann, L. C., & Williams, P. A. (2017). Pectins from food waste:
590 extraction, characterization and properties of watermelon rind pectin. *Food Hydrocolloids*,
591 *65*, 57–67.

592 Ralet, M. C., Dronnet, V., Buchholt, H. C., & Thibault, J. F. (2001). Enzymatically and
593 chemically de-esterified lime pectins: Characterisation, polyelectrolyte behaviour and
594 calcium binding properties. *Carbohydrate Research*, *336*, 117–125.

595 Schmuhl, R., Krieg, H. M., & Keizer, K. (2001). Adsorption of Cu(II) and Cr(VI) ions by
596 chitosan: Kinetics and equilibrium studies. *Water SA*, *27*, 1–7.

597 Shpigelman, A., Kyomugasho, C., Christiaens, S., Van Loey, A. M., & Hendrickx, M. E.
598 (2014). Thermal and high pressure high temperature processes result in distinctly different
599 pectin non-enzymatic conversions. *Food Hydrocolloids*, *39*, 251–263.

600 Slavov, A., Garnier, C., Crépeau, M. J., Durand, S., Thibault, J. F., & Bonnin, E. (2009).
601 Gelation of high methoxy pectin in the presence of pectin methylesterases and calcium.
602 *Carbohydrate Polymers*, *77*(4), 876–884.

603 Sriamornsak, P. (2003). Chemistry of pectin and its pharmaceutical uses: a review. *Silpakorn*
604 *University International Journal*, *3*, 207–228.

605 Ström, A., Ribelles, P., Lundin, L., Norton, I., Morris, E. R., & Williams, M. A. K. (2007).
606 Influence of pectin fine structure on the mechanical properties of calcium - pectin and acid
607 - pectin gels. *Biomacromolecules*, *8*, 2668–2674.

608 Tanhatan-Nasseri, A., Crépeau, M. J., Thibault, J. F., & Ralet, M. C. (2011). Isolation and
609 characterization of model homogalacturonans of tailored methylesterification patterns.
610 *Carbohydrate Polymers*, *86*(3), 1236–1243.

611 Thakur, B. R., Singh, R. K., Handa, A. K., & Rao, M. A. (1997). Chemistry and uses of pectin

- A review. *Critical Reviews in Food Science and Nutrition*, *37*, 47–73.

Thibault, J.-F., & Ralet, M. C. (2003). Physico-chemical properties of pectins in the cel walls and after extraction. In A. G. J. Voragen, H. A. Schols, & R. Visser (Eds.), *Advances in pectin and pectinases research* (pp. 91–105). Dordrecht, The Netherlands: Kluwer Academic Publishers.

Varela, P., & Fiszman, S. M. (2013). Exploring consumers' knowledge and perceptions of hydrocolloids used as food additives and ingredients. *Food Hydrocolloids*, *30*, 477–484.

Viollier, E., Inglett, P. W., Hunter, K., Roychoudhury, A. N., & Van Cappellen, P. (2000). The ferrozine method revisited: Fe(II)/Fe(III) determination in natural waters. *Applied Geochemistry*, *15*, 785–790.

Voragen, A. G. J., Coenen, G. J., Verhoef, R. P., & Schols, H. A. (2009). Pectin, a versatile polysaccharide present in plant cell walls. *Structural Chemistry*, *20*, 263–275.

Wicker, L., Kim, Y., Kim, M. J., Thirkield, B., Lin, Z., & Jung, J. (2014). Pectin as a bioactive polysaccharide - Extracting tailored function from less. *Food Hydrocolloids*, *42*(P2), 251–259.

Willats, W. G. T., Knox, J. P., & Mikkelsen, J. D. (2006). Pectin: New insights into an old polymer are starting to gel. *Trends in Food Science and Technology*, *17*, 97–104.

Willats, W. G. T., Orfila, C., Limberg, G., Buchholt, H. C., Van Alebeek, G. J. W. M., Voragen, A. G. J., … Knox, J. P. (2001). Modulation of the degree and pattern of methyl-esterification of pectic homogalacturonan in plant cell walls: Implications for pectin methyl esterase action, matrix properties, and cell adhesion. *Journal of Biological Chemistry*, *276*(22), 19404–19413.

Yapo, B. M., Lerouge, P., Thibault, J. F., & Ralet, M. C. (2007). Pectins from citrus peel cell walls contain homogalacturonans homogenous with respect to molar mass, rhamnogalacturonan I and rhamnogalacturonan II. *Carbohydrate Polymers*, *69*, 426–435.

Zhao, F., Repo, E., Yin, D., & Sillanpää, M. E. T. (2013). Adsorption of Cd(II) and Pb(II) by a novel EGTA-modified chitosan material: Kinetics and isotherms. *Journal of Colloid and Interface Science*, *409*, 174–182.

Zhao, Z. Y., Liang, L., Fan, X., Yu, Z., Hotchkiss, A. T., Wilk, B. J., & Eliaz, I. (2008). The role of modified citrus pectin as an effective chelator of lead in children hospitalized with

toxic lead levels. *Alternative Therapies*, *14*, 34–38.

Tables

P-pectins			C-pectins		
Sample code	**DM (%)**	**DB_{abs} (%)**	**Sample code**	**DM (%)**	**DB_{abs} (%)**
P69	69.4 ± 1.2	20.6 ± 1.0	**C67**	67.1 ± 0.6	5.1 ± 0.1
P60	59.8 ± 1.4	29.0 ± 1.3	**C46**	45.9 ± 0.5	12.3 ± 0.3
P39	39.2 ± 0.9	49.9 ± 1.0	**C36**	35.9 ± 0.7	20.8 ± 0.8
P33	33.0 ± 2.1	57.1 ± 2.5	**C30**	29.9 ± 0.3	28.1 ± 0.4
P13	13.0 ± 1.3	82.4 ± 1.7	**C20**	20.5 ± 0.4	43.9 ± 0.9

Table 1: DM (%) and estimated DB_{abs} (%) of pectin samples produced by either enzymatic (plant origin, P) or chemical (C) demethylesterification of the mother pectin (M95) ± standard deviations.

Sample code	q^{G}_{max} (mol Fe^{2+}/mol GalA)	q^{C}_{max} (mol Fe^{2+}/mol COO^-)	K_L (L/mmol)	$R^2_{adjusted}$
M95	0.217 ± 0.005 **g**	4.427 ± 0.110 **a**	85.3 ± 14.9 **de**	0.99
P69	0.253 ± 0.004 **f**	0.826 ± 0.013 **b**	146.0 ± 16.3 **cd**	0.99
P60	0.309 ± 0.006 **e**	0.768 ± 0.013 **cd**	190.3 ± 26.4 **c**	0.99
P39	0.429 ± 0.015 **bc**	0.705 ± 0.025 **de**	473.6 ± 104.1 **ab**	0.98
P33	0.463 ± 0.011 **b**	0.692 ± 0.017 **e**	351.0 ± 42.9 **a**	0.99
P13	0.523 ± 0.010 **a**	0.602 ± 0.012 **f**	399.1 ± 40.8 **a**	0.99
C67	0.191 ± 0.004 **h**	0.582 ± 0.012 **fg**	78.7 ± 9.9 **e**	0.99
C46	0.270 ± 0.005 **f**	0.499 ± 0.010 **h**	195.2 ± 31.1 **bc**	0.99
C36	0.372 ± 0.011 **d**	0.580 ± 0.017 **fg**	128.8 ± 23.3 **cde**	0.99
C30	0.401 ± 0.010 **cd**	0.572 ± 0.014 **fg**	118.8 ± 17.6 **cde**	0.99
C20	0.427 ± 0.009 **bc**	0.537 ± 0.011 **gh**	179.6 ± 22.0 **c**	0.99

Table 2: Parameter estimates ± standard deviation for Langmuir adsorption isotherms of different pectin samples. q^{G}_{max} is the maximum binding capacity, expressed as mol Fe^{2+}/mol GalA and q^{C}_{max} the maximum binding capacity, expressed as mol Fe^{2+}/mol COO^-. K_L (L/mmol) represents the adsorption energy. The letters (a-h) indicate significantly different values at a 95% confidence interval.

Figures

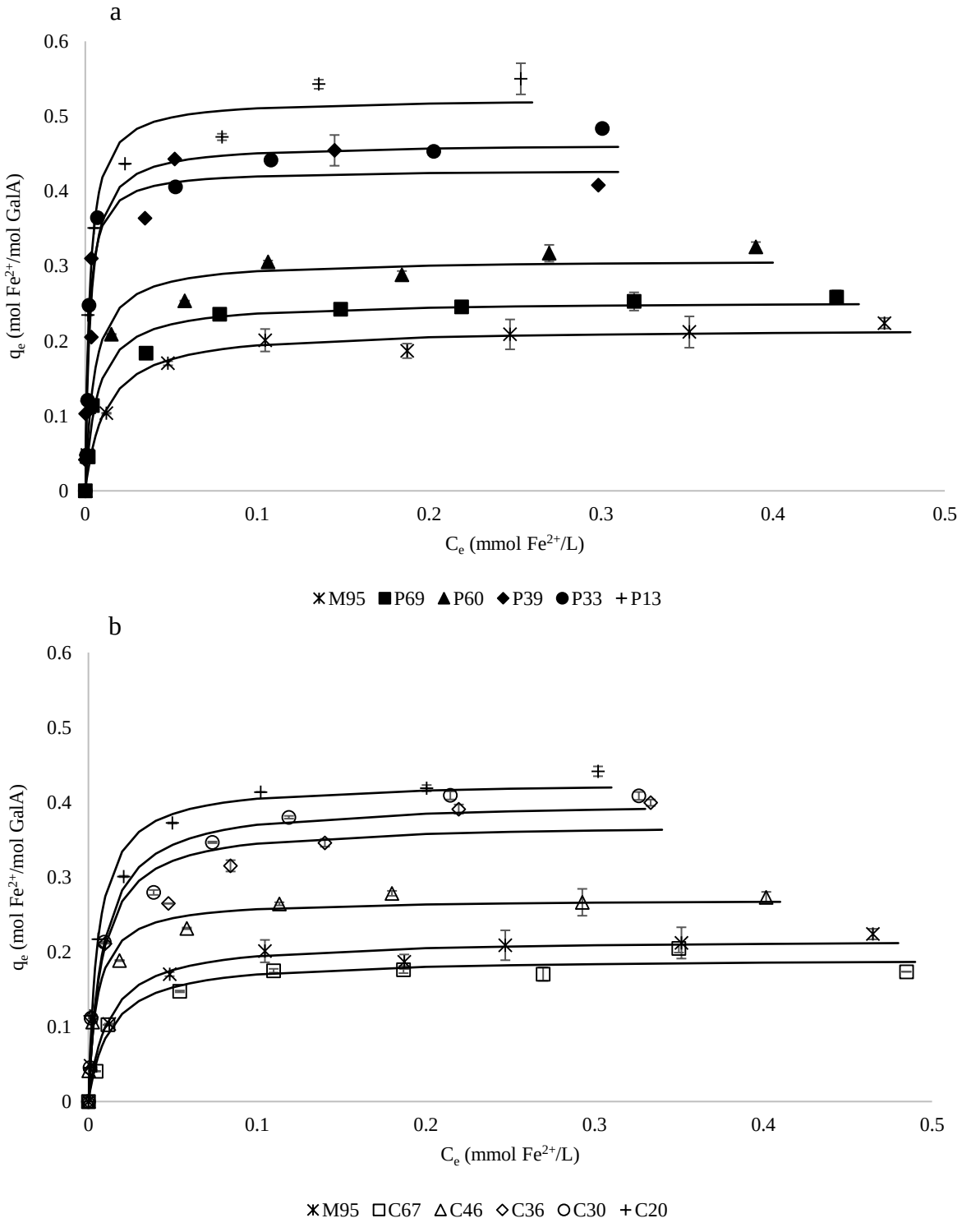

Figure 1: Adsorption isotherms representing q_e (mol Fe^{2+}/mol GalA) in function of Fe^{2+} equilibrium concentration (mmol/L) for a) P-pectins with different DMs and b) C-pectins with different DMs. Symbols indicate the experimental data ± standard deviation. Black curves are modeled Langmuir adsorption isotherms.

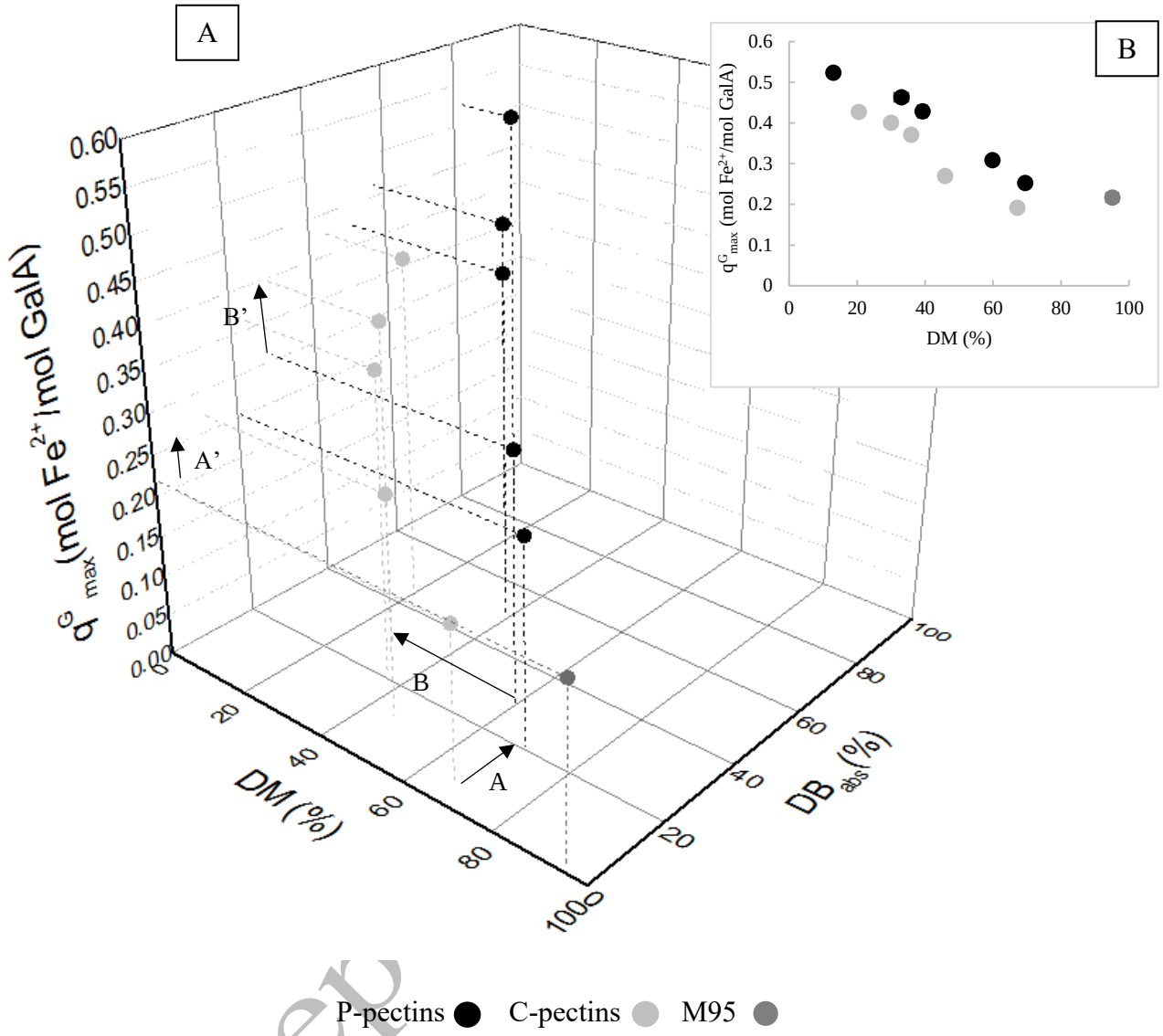

Figure 2: a) q^G_{max} (mol Fe^{2+}/mol GalA) of P- and C-pectins as a function of DM (%) and DB_{abs} (%) and b) relation between q^G_{max} (mol Fe^{2+}/mol GalA) ± standard deviation and DM of P- and C-pectins.

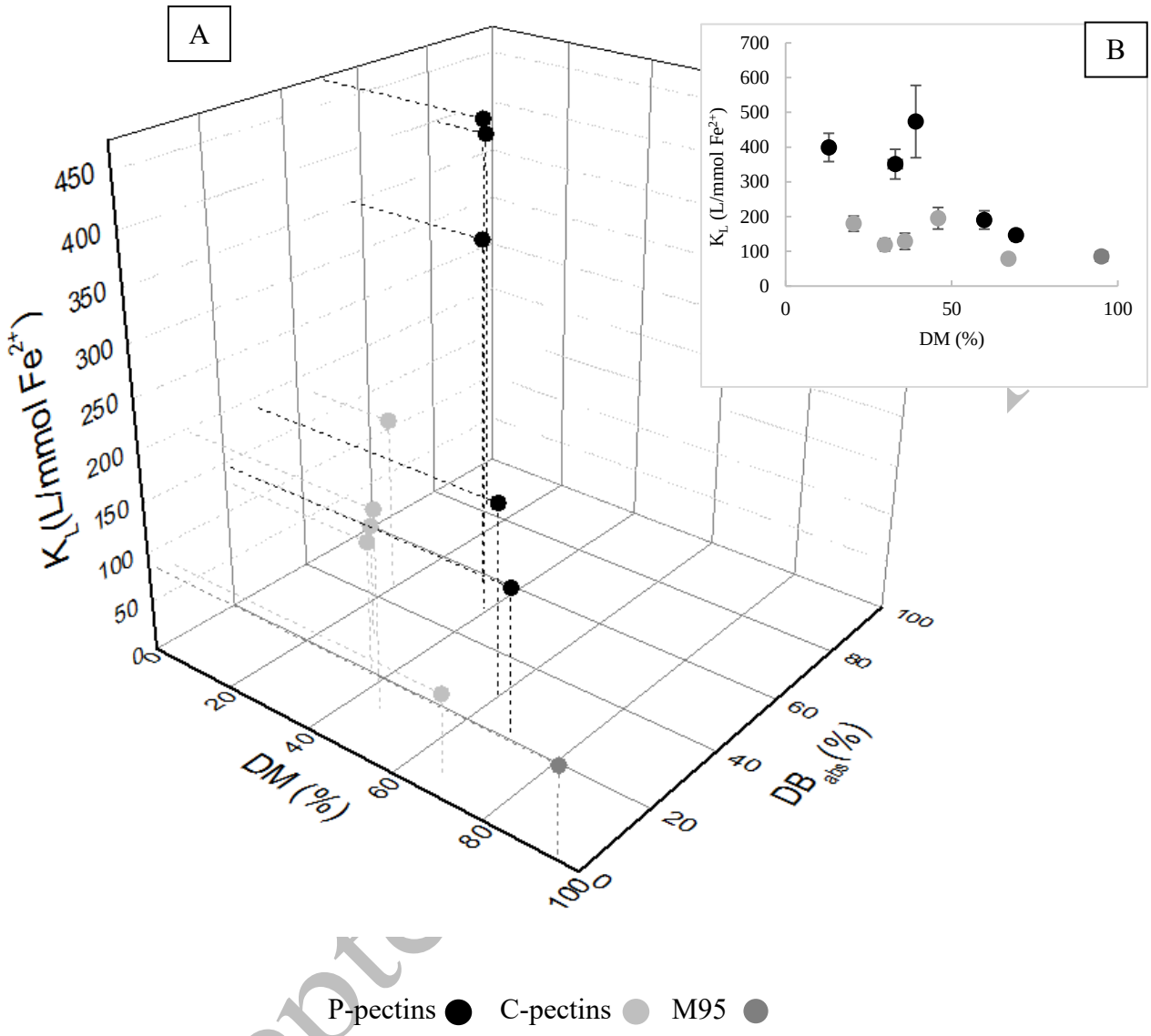

Figure 3: a) K_L (L/mmol Fe^{2+}) of P- and C-pectins as a function of DM (%) and DB_{abs} (%) and b) relation between K_L (L/mmol Fe^{2+})± standard deviation and DM of P- and C-pectins.

753

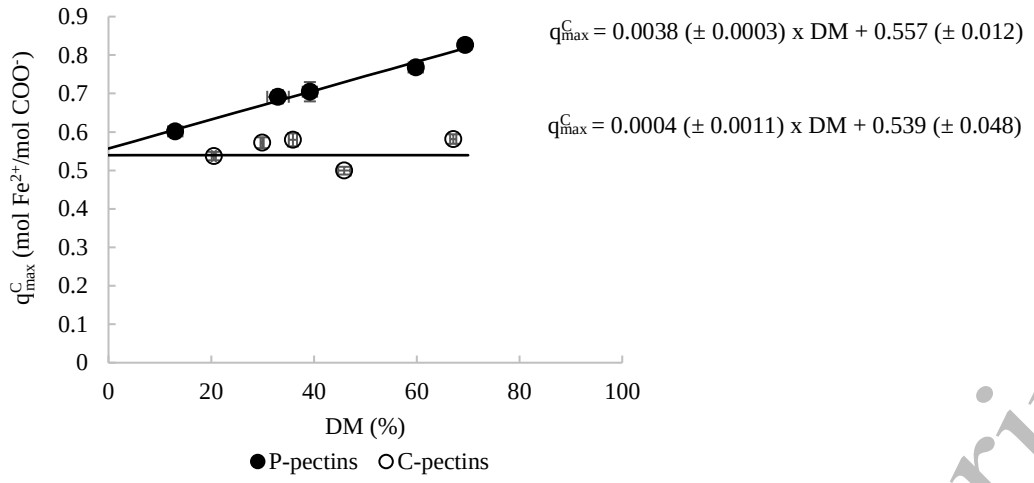

754

755

756 *Figure 4: q^{C}_{max} (mol Fe^{2+}/mol COO^-) of P- and C-pectins as a function of DM (%). Symbols indicate the estimated q^{C}_{max} values*
757 *± standard deviation. Black curves represent linear models with associated equations.*

758

759

760